

New BaCoO_{3-δ} Polytypes by Rational Substitution of O²⁻ for F⁻

Ghislaine Ehora, Catherine Renard,
Sylvie Daviero-Minaud, and Olivier Mentré*

Unité de Catalyse et de Chimie du Solide, Equipe de Chimie
du Solide UMR-CNRS- 8181, USTL/ENSCL, bât. C7,
59652 Villeneuve d'Ascq Cedex, France

Received March 1, 2007

Revised Manuscript Received April 27, 2007

State of the Art. Chemical rules available to modify target compounds and/or create new crystal structures with respect to a predicted route are strongly attractive for solid-state chemists. Unfortunately, in this field, the rational design of new structural types remain rarely reliable, leading to a number of exceptional cases or unpredicted behaviors. Especially, several “exotic” structural types appear of great interest, but paradoxically often do not fit predictive criteria. Here, we report the modification of the stacking of anionic layers among the wide series of hexagonal perovskite oxides, using the selective substitution of oxide for monovalent anions.

At the basis of the search for original electronic and magnetic behavior, a number of studies focus on the prospecting for new complex structural types within “hot” topics such as cobaltite (strong competition between magnetic ground states, attractive thermoelectricity,¹ superconductivity,² etc.). In the field of perovskite-related oxide materials, the calculation of the well-known Goldschmidt tolerance factor (*t*) remarkably well anticipates possible distortion from the 3C ideal cubic-type.³ However, it mostly concerns compounds built on the stacking of ideal [AO₃] anionic layers, and as a matter of fact depends on both the ionic radii of A, O and B, the interstitial cation. As soon as deficient anionic layers are involved, the stacking type gets ruled out by a number of hardly estimable parameters. The examination of the BaCoO_{3-δ} series exemplifies well this inability for structural prediction. For δ = 0, the 2H form is stabilized where the hexagonal (h) packing of every layer is predicted by *t* > 1. Two additional forms have been reported so far, the 5H form for δ ≈ 0.26⁴ and the 12H form for δ ≈ 0.4.⁵ In both of them, oxygen-deficient [BaO_{3-x}] layers still respect the h packing and create trimers or tetramers of face-sharing octahedra. However, in between them, lacunar cubic (c) [BaO₂] layers create isolated tetrahedra, leading to

(hhhcc'c)₂ and (hhcc'c) sequences in the 12H and 5H polymorphs, respectively, where c/h and c' denote [BaO₃] and [BaO₂] layers, see images a and b in Figure 1.

The basis of our work comes from the simple comparison between these two structural types and the modified structures reported for the 5H BaFeO_{2.8} and BaFeO_{2.65} with the (chchh) stacking sequence.⁶ They both contain octahedral trimers isolated by Fe₂O₇ pairs of corner-sharing tetrahedra at both sides of the h [BaO₂] layer. However, the orthorhombic distortion reported in ref 6b for the latter remains unclear as compared to the hexagonal form for the former.^{6a} In these compounds, the central h [BaO₂] layer contains an underbonded O²⁻ anion pentacoordinated by Ba²⁺ cations, i.e., the valence-bond sums (BVS) are -0.63 and -0.46, respectively, instead of -2 using O'Keefe data.⁷ It strongly suggests the likely presence of a monovalent anion, with regard to a more favorable BVS. At this point, it is noteworthy that OH⁻ and Cl⁻ are involved during the synthesis of BaFeO_{2.8} (Ba(OH)₂/KOH flux) and BaFeO_{2.65} (thermal decomposition of BaFe[(CN)₅NO] prepared in a prior stage using BaCl₂ as an exchanging agent). It would yield more reasonable BVS values, i.e., -0.63 for OH⁻ and -1.36 for Cl⁻, in h [BaOX] layers.

From this observation, the possible modification of the 5H and 12H BaCoO_{3-δ} forms into the new (ch'chh)-based Ba₅Co₅FO_{13-δ} (**1**) and (ch'chhh) Ba₆Co₆FO_{16-δ} (**2**) has been imagined. The method is based on the predicted preference of monovalent anions for Ba pentacoordination, leading to a shearing of the cubic [BaO₂] into an hexagonal [BaOX] layer. Both materials have been prepared as single crystals/single-phased powders and characterized; see the Supporting Information for further details. Their feasibility was reinforced by the prior existence of the chloride isotopes,⁸ whereas the replacement of voluminous and structuring Cl⁻ species by smaller and interstitial F⁻ was expected to be responsible for important structural distortions. The crystal structures of the two prepared Ba/Co oxyfluorides as refined from single-crystal X-ray diffraction (XRD) data are shown in images c and d of Figure 1. (10H polytype, **1**): hexagonal *a* = 5.6878(5) Å, *c* = 23.701(5) Å, *P*6₃/*mmc*, *R*₁ = 2.72%, *wR*₂ = 5.44%, *n*_{ref} = 368; 6H polytype, **2**): hexagonal *a* = 5.6683(5) Å, *c* = 14.277(3) Å, *P*6*m*2, *R*₁ = 1.60%, *wR*₂ = 3.46%, *n*_{ref} = 415). The connection by corners of the isolated blocks of the two BaCoO_{3-δ} polymorphs into 3D structures appears rather exciting from the point of view of the physical properties.

Structural Features. The size of the building blocks are nearly unchanged from the oxides to the oxyfluorides, such

* To whom correspondence should be addressed. E-mail: olivier.mentre@ensc-lille.fr.

- (1) Terasaki, I.; Sasago, Y.; Uchinokura, K. *Phys Rev. B* **1997**, *56*, R12685.
- (2) Takeda, K.; Sakurai, H.; Takayama-Murimachi, E.; Izumi, F.; Dilanian, R. A.; Sasaki, T. *Nature* **2003**, *422*, 53.
- (3) (a) Glazer, A. M. *Acta Crystallogr., Sect. B* **1972**, *28*, 3384. (b) O'Keefe, M.; Hyde, B. G. *Acta Crystallogr., Sect. B* **1977**, *33*, 3802.
- (4) (a) Parras, M.; Varela, A.; Seehofer, H.; Gonzalez-Calbet, J. M. *J. Solid State Chem.* **1995**, *120*, 327. (b) Boulahya, K.; Parras, M.; Gonzalez-Calbet, J. M.; Amador, U.; Martinez, J. L.; Tissen, V.; Fernandez-Diaz, M. T. *Phys. Rev. B* **2005**, *71*, 144402.
- (5) (a) Jacobson, A. J.; Hutchison, J. L. *J. Solid State Chem.* **1980**, *35*, 334. (b) Hector, A. L.; Hutchings, J. A.; Needs, R. L.; Thomas, M. F.; Weller, T. *J. Mater. Chem.* **2001**, *11*, 527.

- (6) (a) Gomez, M. I.; Lucotti, G.; de Moran, J. A.; Aymonimo, J. M.; Pagola, S.; Stephens, P.; Carbonio, R. E. *J. Solid State Chem.* **2001**, *160*, 17. (b) Delattre, J. L.; Stacy, A. M.; Siegrist, T. *J. Solid State Chem.* **2004**, *177*, 928.
- (7) Bresse, N. E.; O'Keefe, M. *Acta Crystallogr., Sect. B* **1991**, *47*, 192.
- (8) (a) Yamamura, K.; Young, D. P.; Siegrist, T.; Besnard, C.; Svensson, C.; Liu, Y.; Cava, R. J. *J. Solid State Chem.* **2001**, *158*, 175. (b) Tancret, N.; Roussel, P.; Abraham, F. *J. Solid State Chem.* **2005**, *178*, 3066.

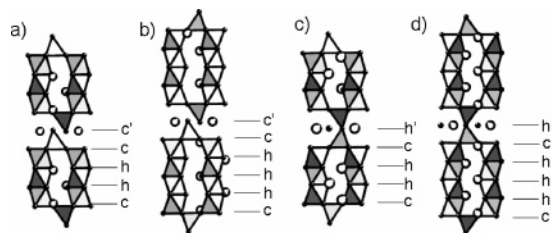


Figure 1. Structural view of (a) the 5H form and (b) 12 H form of $\text{BaCoO}_{3-\delta}$, (c) $\text{Ba}_5\text{Co}_5\text{FO}_{13-\delta}$, and (d) $\text{Ba}_6\text{Co}_6\text{FO}_{16-\delta}$.

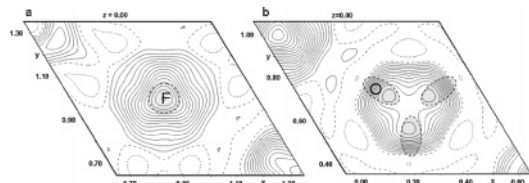


Figure 2. Electronic density layers for $\text{Ba}_6\text{Co}_6\text{FO}_{16-\delta}$ at $z = 0$ without the anions of the [BaOF] layers. It shows (a) the spherical shape of the F anion (b) the split of the oxygen in the layers.

that the [BaOX] layers appear as likely shearing planes with no extra structural perturbation. Surprisingly, the comparison between the lattice parameters and bond distances of the oxyfluorides and the oxychlorides reveals that the structure adapts itself to the X species by a dilatation of the c lattice parameter only. It is pictured by a drastic change of the apical Ba–X distances for Cl^- (2.94–2.96 Å) and F^- (2.66–2.71 Å). This effect is particularly interesting in terms of the induced “chemical pressure” well-known to influence the cobalt spin states. Once more, should we also mention that the apical Ba–X distances of 3.01 and 2.89 Å in $\text{BaFeO}_{2.65}$ and $\text{BaFeO}_{2.8}$ ⁶ appear nicely compatible with the possible true formulas $\text{Ba}_3\text{Fe}_5(\text{Cl})\text{O}_{12.25}$ and $\text{Ba}_3\text{Fe}_5(\text{OH})\text{O}_{13}$ suggested above.

One of the key points of this work is to establish the preference of the [BaOX] layer ($X = \text{OH}^-, \text{F}^-, \text{Cl}^-$, etc.) for hexagonal packing able to modify cubic [BaO₂] layers by selective O for X substitution on the pertinent anionic site. However, even if BVS comforts the observed stacking sequences considering F^- in its assumed position, it is well-known that fluorides can occupy multiple sites in the structure (replacement of oxygen vacancies for instance) or even be volatilized during the thermal treatment. First, it is essential to know that our attempts to prepare (1) and (2) without any F precursor in the same conditions led to a mixture of $\text{BaCoO}_{3-\delta}$ forms. In addition, the titration of F^- has been performed using a specific electrode and leads to the expected values, 0.9(3) and 1.0(3) per formula unit, respectively. However, its location in [BaOX] layers cannot be proved by diffraction techniques considering the poor fluor/oxygen contrast from XRD as well as ND. In this aim, the DFT calculations presented below comforts the validity of our model.

In both (1) and (2), the oxygen atom of the [BaOF] layer is split around the central special position, whereas the fluoride shows a spherical electronic density, as shown on the Fourier difference map, Figure 2. It could be due to the overbonded character of the in-plane Ba atom, whereas the oxygen off-centering modifies its BVS from 1.56 to 1.73 (1) and from 1.64 to 1.72 (2). A similar splitting has already been reported for $\text{Ba}_6\text{Co}_6\text{ClO}_{16-\delta}$.^{8b}

Table 1. Interatomic Distances (Å) and Calculated Bond-Valence Sums (Σs_{ij}) of Cobalt Atoms (+3 Hypothesis) in $\text{Ba}_6\text{Co}_6\text{O}_{16-\delta}$ and $\text{Ba}_5\text{Co}_5\text{O}_{13-\delta}$

| $\text{Ba}_6\text{Co}_6\text{FO}_{15.5}$ | | $\text{Ba}_5\text{Co}_5\text{FO}_{13}$ | |
|--|-----------|--|-----------|
| Co O octahedra | d (Å) | Co O octahedra | d (Å) |
| Co1–O1($\times 3$) | 1.9146(5) | Co1–O1($\times 3$) | 1.9274(6) |
| Co1–O2($\times 3$) | 1.9376(6) | Co1–O2($\times 3$) | 1.9464(5) |
| $\Sigma s_{ij} = 3.26$ | | $\Sigma s_{ij} = 3.16$ | |
| Co2–O1($\times 3$) | 1.8903(5) | Co2–O2($\times 6$) | 1.8916(5) |
| Co2–O3($\times 3$) | 1.9002(6) | | |
| $\Sigma s_{ij} = 3.54$ | | $\Sigma s_{ij} = 3.57$ | |
| Co O tetrahedra | d (Å) | Co O tetrahedra | d (Å) |
| Co3–O4($\times 1$) | 1.7786(1) | Co3–O3($\times 1$) | 1.869(1) |
| Co3–O2($\times 3$) | 1.8105(6) | Co3–O1($\times 3$) | 1.8277(6) |
| $\Sigma s_{ij} = 3.78$ | | $\Sigma s_{ij} = 3.42$ | |

In the $\text{BaCoO}_{3-\delta}$ series, tetrahedral Co^{IV} and both octahedral Co^{III} and mixed octahedral $\text{Co}^{\text{III}}/\text{Co}^{\text{IV}}$ have been suggested, depending on the δ value. In the two oxyfluorides, both the redox titration (see the Supporting Information) and the analogy with $\text{Ba}_6\text{Co}_6\text{ClO}_{16}$ ⁹ indicate a global $\text{Co}^{\text{III}}/\text{Co}^{\text{IV}}$ charge ordering in octahedral and tetrahedral sites, respectively, in agreement with the exact formulas $\text{Ba}_5\text{Co}^{\text{III}}_3\text{Co}^{\text{IV}}_2\text{FO}_{13}$ and $\text{Ba}_6\text{Co}^{\text{III}}_4\text{Co}^{\text{IV}}_2\text{FO}_{15.5}$. In addition, the Co–O distances and BVS for Co^{III} are calculated between +3.16 and +3.57, as commonly observed in Co^{III} oligomers,¹⁰ whereas tetrahedral $\text{Co}^{\text{IV}}\text{–O}$ distances are consistent with those of $\text{BaCoO}_{3-\delta}$. According to the susceptibility measurements (see the Supporting Information) and the neutron diffraction (ND) data to be published in a further work, both compounds show a paramagnetic \rightarrow antiferromagnetic transition on cooling: (1) $\mu_{\text{eff}} = 6.97 \mu\text{B/f.u.}$, $\theta = -311 \text{ K}$, $T_{\text{N}} = 122 \text{ K}$; (2) $\mu_{\text{eff}} = 6.82 \mu\text{B/f.u.}$, $\theta = -278 \text{ K}$, $T_{\text{N}} = 126 \text{ K}$. It is explained by low-spin Co^{III} ($S = 0$) and intermediate tetrahedral Co^{IV} ($e_g^3 t_{2g}^2$; $S = 3/2$, $\mu_{\text{eff}}^{\text{spin-only}} = 5.47 \mu\text{B/f.u.}$) with a certain amount of spin–orbit coupling contribution. Here, a so-called intermediate spin-state for Co^{IV} may result from the particular crystal-field splitting arising from the tetrahedral distortion discussed above.

DFT Calculations. Four models derived from (2) (connected tetrameric blocks) and $\text{BaCoO}_{\sim 2.6}$ (disconnected tetrameric blocks) have been simulated, playing on the [BaO₂] or [BaOF] nature of the central layer. The ab initio calculations were performed within density functional theory using VASP code,¹¹ employing a plane wave basis set as detailed in the Supporting Information. The Kohn–Sham equations were solved using the generalized gradient approximation (GGA) functionals for exchange and correlation.¹² The core electrons were treated using the plane-augmented wave (PAW)¹³ approach. The c parameter of the 6H structure was doubled in order to consider the same cell volume for all the models. The experimental atomic positions

- (9) Kauffmann, M.; Mentré, O.; Legris, A.; Tancret, N.; Abraham, F.; Roussel, P. *Phys. Rev. Lett.* **2006**, *432*, 88.
 (10) (a) Sun, J.; Yang, M.; Li, G.; Yang, T.; Liao, F.; Wang, Y.; Xiong, M.; Lin, J. *Inorg. Chem.* **2006**, *45* (23), 9151. (b) Ehora, G.; Daviero-Minaud, S.; Colmont, M.; André, G.; Mentré, O. *Chem. Mater.* **2007**, *19*, 2180.
 (11) (a) Kresse, G.; Hafner, J. *Phys. Rev. B* **1994**, *49* (14), 251. (b) Kresse, G.; Furthmüller, J. *Comput. Mater. Sci.* **1996**, *6*, 15. (c) Kresse, G.; Furthmüller, J. *Phys. Rev. B* **1996**, *54* (11), 169.
 (12) Perdew, J. P.; Wang, Y. *Phys. Rev. B* **1992**, *45*, 13244.
 (13) Kresse, G.; Joubert, J. *Phys. Rev. B* **1999**, *59*.

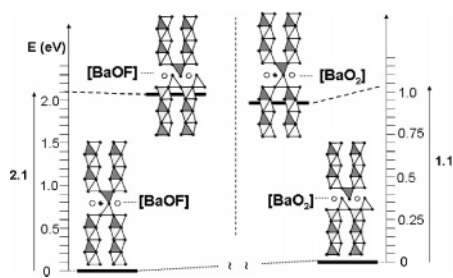


Figure 3. Diagram of the total energy of the existing and hypothetical oxides and oxyfluorides systems with tetrameric units.

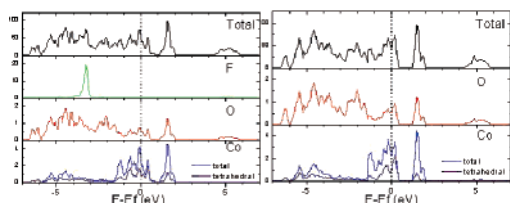


Figure 4. DOS and PDOS for $\text{Ba}_6\text{Co}_6\text{O}_{16}\text{F}$ and $\text{Ba}_6\text{Co}_6\text{O}_{17}$ (units: states (eV/unit cell) and states (eV/atom) for total and partial density of state).

and cell parameters of $\text{BaCo}_2\text{O}_{2.6}$ and $\text{Ba}_6\text{Co}_6\text{FO}_{15.5}$ were used as initial data. No partial oxygen site occupancy was introduced. The relative structure stabilities of the two oxides on the one hand and the two oxyfluorides on the other are evaluated, comparing the values of total energy. For the two realistic tested models, the structure relaxation shows that the optimized cell parameters are slightly overestimated, by 0.4% and from 1.1 to 1.4% for a and c , respectively, which is the usual trend for GGA.

Oxides. The geometrical optimization of the hypothetical connected $\text{Ba}_6\text{Co}_6\text{O}_{17}$ structure leaves the cell unchanged. However, for the latter, it is noteworthy that the displacement of the apical Ba toward the central O^{2-} leads to abnormally short Ba–O distances of 2.52 Å. The disconnected structure is undoubtedly the most stable form, because the total energy is 0.58 eV lower per 6 Ba-containing f.u., in good agreement with the reported structure.

Oxyfluorides. In the hypothetical disconnected $\text{Ba}_6\text{Co}_6\text{O}_{16}\text{F}$ structure, the fluoride ions replace one apex of the CoO_4 tetrahedron. Its relaxation yields a large displacement of F^- away from the basal O_3 opposite face and an elongation of the c parameter. Hence the Co–F distance is rather long, 2.38 Å. The structural model corresponding to (2) is more stable than the disconnected polytype, with an energy difference of 1.06 eV/f.u. (Figure 3). Our calculations then unambiguously confirm the preference of halides and oxides for hexagonal and cubic packing, respectively, and validate our structural models.

The comparison of the density of states (DOS) and the partial DOS (PDOS) of the two stable compounds is shown in Figure 4. The aim of this section is not explore the detailed electronic structure of both compounds, already discussed for $\text{Ba}_6\text{Co}_6\text{O}_{16}\text{Cl}$,⁹ but rather to estimate the effect of the shearing of the [BaOX] layer. Then three main effects can be deduced.

(i) Both compounds show a metallic behavior with comparable valence bands mainly formed from formed O_{2p} and Co_{3d} levels. However, the disconnection of the elementary blocks yields the creation of a 0.8 eV gap instead of the preliminary pseudo-gap up to antibonding levels.

(ii) The broadening of the valence band in the connected structure is due to the contribution of tetrahedral cobalt and their oxygen apex as evidenced by PDOS. This illustrates rather well the cutting of the 3D structure into 2D blocks.

(iii) The 2p-like states of F form a thin isolated band (bandwidth ~ 0.7 eV) in agreement with its predominantly bonding ionic character, stabilized by its surrounding Ba^{2+} cations only.

Because of its effect on the cationic valence, fluorination has been performed on cuprates, Ruddlesden–Popper, and related materials.¹⁴ They generally lead to substitution/insertion with two F^- replacing one O^{2-} , whereas F^- are commonly located in the rocksalt layers. For perovskite materials, fluorination mainly focuses on brownmillerite-like oxygen-deficient compounds leading the (partial) filling of vacancies, with possible local O/F/ \square ordering.¹⁵ Here, we have shown that the rational substitution of O for F in cubic deficient $[\text{BaO}_2]$ layers appears as a promising route to new materials. The limits of the method are intrinsic to the target compound: tetrahedral species should be able to adopt isolated TO_4 and corner-sharing T_2O_7 groups ($\text{T} = \text{Co}^{\text{IV}}, \text{Al}^{\text{III}}, \text{V}^{\text{V}} \dots$), whereas the framework should bear the reduction process associated with the X^- for O^{2-} replacement, e.g., $[\text{octaCo}^{\text{III/IV}}]_{\text{BaCoO}_{3-d}} \rightarrow [\text{octaCo}^{\text{III}}]_{\text{BaCo}(\text{O},\text{F})_{3-d}}$. Aliovalent substitutions within the framework may honor the electroneutrality as well.

Acknowledgment. We thank Dr P. Roussel and M. Kauffmann for informative discussion.

Supporting Information Available: Experimental details and other relevant data (PDF); crystallographic information for the two crystal structures in CIF format. This material is available free of charge via the Internet at <http://pubs.acs.org>.

CM070576O

- (14) (a) Hector, A. L.; Hutchings, J. A.; Needs, R. L.; Thomas, M. F.; Weller, M. T. *J. Mater. Chem.* **2001**, *11*, 527. (b) Case, G. S.; Hector, A. L.; Levason, W.; Needs, R. L.; Thomas, M. F.; Weller, M. T. *J. Mater. Chem.* **1999**, *9*, 2821. (c) Slater, P. R.; Gover, R. K. B. *J. Mater. Chem.* **2002**, *12*, 291. (d) Hadermann, J.; Abakumov, A. M.; Lebedev, O. I.; Van Tendeloo, G.; Rozova, M. G.; Shapanchenko, R. V.; Pavlyuk, B. P.; Kopnin, E. M.; Antipov, E. V. *J. Solid State Chem.* **1999**, *147*, 647. (e) Hadermann, J.; Khasanova, N. R.; Van Tendeloo, G.; Abakumov, A. M.; Rozova, M. G.; Alekseeva, A. M.; Antipov, E. V. *J. Solid State Chem.* **2001**, *156*, 445.
- (15) (a) Abakumov, A. M.; Hadermann, J.; Rozova, M. G.; Pavlyuk, B. P.; Antipov, E. V.; Lebedev, O. I.; Van Tendeloo, G. *J. Solid State Chem.* **2000**, *149*, 189. (b) Hadermann, J.; Van Tendeloo, G.; Abakumov, A. M.; Pavlyuk, B. P.; Rozova, M.; Antipov, E. V. *Int. J. Inorg. Mater.* **2000**, *2*, 493. (c) Berry, F. J.; Ren, X.; Slater, P.; Thomas, M. F. *Solid State Commun.* **2005**, *134*, 621.